

CONF-9508210--1

RECEIVED

FEB 08 1986

OSTI

RHIC Spin Program

G. BUNCE

*Brookhaven National Laboratory
Upton, New York 11973-5000, USA*

Introduction

Colliding beams of high energy polarized protons at RHIC is an excellent way to probe the polarization of gluons, u and \bar{d} quarks in a polarized proton. RHIC is the Relativistic Heavy Ion Collider being built now at Brookhaven in the ISABELLE tunnel. It is designed to collide gold ions on gold ions at 100 GeV/nucleon. Its goal is to discover the quark-gluon plasma, and the first collisions are expected in March, 1999.

RHIC will also make an ideal polarized proton collider with high luminosity and 250 GeV x 250 GeV collisions. The RHIC spin physics program is:

1. Use well-understood perturbative QCD probes to study non-perturbative confining dynamics in QCD. We will measure
 - gluon and sea quark polarization in a polarized proton,
 - polarization of quarks in a transversely polarized proton.
2. Look for additional surprises using the first high energy polarized proton collider. We will
 - look for the expected maximal parity violation in W and Z boson production,
 - search for parity violation in other processes,
 - test parton models with spin.

This lecture is organized around a few of the key ideas:

- Siberian Snakes--What are they?
- High energy proton-proton collisions are scatters of quarks and leptons.
- at high x , a polarized proton beam is a beam of polarized u quarks.
- quark and gluon collisions are very sensitive to spin.

We will discuss two reactions: how direct photon production measures gluon polarization, and how W^+ boson production measures u and \bar{d} quark polarization.

Siberian Snakes

It is very difficult to accelerate polarized particles in a circular accelerator. Any horizontal magnetic field encountered during acceleration readily tips the spin away from vertical. Depolarizing resonances occur when these perturbations beat with a frequency which matches the spin rotation around the guide field of the accelerator.

DISCLAIMER

This report was prepared as an account of work sponsored by an agency of the United States Government. Neither the United States Government nor any agency thereof, nor any of their employees, makes any warranty, express or implied, or assumes any legal liability or responsibility for the accuracy, completeness, or usefulness of any information, apparatus, product, or process disclosed, or represents that its use would not infringe privately owned rights. Reference herein to any specific commercial product, process, or service by trade name, trademark, manufacturer, or otherwise does not necessarily constitute or imply its endorsement, recommendation, or favoring by the United States Government or any agency thereof. The views and opinions of authors expressed herein do not necessarily state or reflect those of the United States Government or any agency thereof.

MASTER

This is shown in Figure 1. After the proton passes through the region with horizontal field, its spin is tipped by $\Delta\theta$ in a vertical plane perpendicular to the radial direction. The proton spin then precesses around the vertical guide field by $\frac{(\epsilon-2)}{2}$ faster than the cyclotron frequency of the proton where $\frac{(\epsilon-2)}{2}$ is the anomalous magnetic moment, 1.79, and γ is the Lorentz factor E/m . Resonance occurs when the spin precesses back to the vertical plane, so that the second pass through the horizontal magnetic field then doubles the tilt of the spin.

In the lecture, I compared this to the resonance which destroyed the Tacoma Rapids Suspension Bridge in 1940. Gusting wind had matched the frequency of the bridge suspenders, driving it into a resonance.

The solution for future bridges was to go back to the cross ties of the suspenders used on the Brooklyn Bridge (built 70 years earlier) or tying the decks so that one area of the bridge doesn't have a resonant frequency. This could be analogous to accelerating particles with different g-2 values--not a very useful solution for accelerating polarized protons.

The Siberian solution for accelerating particles is to reverse the y-component of the spin on each pass. Then, as shown in Figure 1c, any perturbation will be canceled on the second pass. This doesn't work well for bridges!

This idea was from Derbenev and Kondratenko, in 1976 at BINP, Novosibirsk.¹ The most obvious way to reverse the y component of the spin is to use a solenoid. However, the spin precession has a $1/\gamma$ factor so that it quickly becomes impractical at higher energies. A solenoid was used to study the Siberian Snake idea at the Indiana cyclotron, confirming the technique.² For RHIC, a series of dipole magnets will be used to reverse the y-component of the spin and leave the beam on axis.

The term "snake" came from the twisting trajectory that the beam follows while passing through the magnets.

Figure 2 shows the snake we will build for RHIC, using four helical dipoles. The idea of using helical dipoles in this way is from Y. Shatunov and V. Ptitsin in 1993.³ The figure shows the field, the beam excursions, and the spin components for protons. Each dipole is one complete helix. A model is being constructed now at Brookhaven.

We have also installed a "partial Siberian Snake" in the AGS and tested it. By introducing a rotation of the spin of less than π , one can decouple weaker resonances. The AGS does not have the space for a full snake, and Thomas Roser proposed this instead.⁴ In our tests so far, the partial snake works as expected (this technique had been used at VEPP-2M for electrons¹--this was the first use of the partial snake), crossing about 40 resonances in the AGS.⁵ This snake does not work for resonances caused by quadrupole focusing (as was known), however, and we will use sudden changes in the focusing to "jump" these intrinsic resonances.

We expect to achieve 70% polarized proton beams in RHIC.

Figure 3 shows the RHIC polarized proton complex. All the spin hardware

through the AGS is installed and working. Snakes and spin rotators (to give longitudinal polarization) are need for RHIC, and a RHIC polarimeter for each beam.

Scattering Quarks and Gluons

At high transverse momentum p_T , hadrons are beams of well-understood quarks and gluons. The advantage of hadron probes over leptons is that quarks and gluons can "see" the gluons in the "target" directly so that gluon polarization can be measured; also parity violation in W^\pm production gives direct measures of tagged u, \bar{d} (W^+) and d, \bar{u} (W^-) polarization in the polarized proton.

At high energy ($\sqrt{s} = 500$ GeV) and high luminosity ($L = 2 \times 10^{32} \text{ cm}^{-2} \text{ sec}^{-1}$), there will be copious production of, for example, direct photons for $p_T > 10 \text{ GeV}/c$ and jets for $p_T > 50 \text{ GeV}/c$. For these large p_T reactions, the parton model applies and the cross section factors as shown in Figure 4.⁶ This leads to a simple relationship for asymmetry. For the case where both beams are longitudinally polarized, the 2-spin asymmetry A_{LL} , defined as the difference of spin parallel minus antiparallel cross sections divided by the sum, normalized to the beam polarizations P_1 and P_2 ,

$$A_{LL} = \frac{1}{P_1 P_2} \frac{N(\uparrow\uparrow) - N(\uparrow\downarrow)}{N(\uparrow\uparrow) + N(\uparrow\downarrow)} \quad (1)$$

then

$$A_{LL} = \frac{\Delta a}{a} \frac{\Delta b}{b} \hat{a} (a + b - c + d). \quad (2)$$

a and b are the incident partons, and $\frac{\Delta a}{a}$ ($\frac{\Delta b}{b}$) is the polarization of parton a(b). \hat{a} is the subprocess analyzing power for a + b - c + d. This is the difference over the sum of the subprocess spin-dependent cross sections:

$$\hat{a} = \frac{d\hat{\sigma}_{++} - d\hat{\sigma}_{+-}}{\text{sum}} \quad (3)$$

This represents the analyzing power for a particular reaction at the quark/gluon level. For the lowest order Feynman graphs for most quark and gluon processes, this ana-

lyzing power is large. This results in the sensitivity for proton-proton collisions to spin.

The sensitivity to spin, the large subprocess analyzing powers a , is from angular momentum conservation and from the inhibition of helicity flip for massless quarks. An example is subprocess $g + g \rightarrow q + \bar{q}$. If the initial gluons have opposite helicity, $J_z = 0$ initially, and the $q\bar{q}$ pair can also give $J_z = 0$. However, if the gluons have the same helicity, $J_z = 2$, and the $q\bar{q}$ pair cannot be produced and conserve angular momentum. Therefore, from equation 3, $a = -1$. This subprocess has - 100% analyzing power.

Figure 5 shows the subprocess analyzing power for many subprocesses. To take one example, direct photon production for proton-proton collisions is dominated by the Compton graph $g + q \rightarrow q + \gamma$, shown in Figure 6 (the annihilation graph $q\bar{q} \rightarrow g\gamma$ is a factor of ten smaller for proton-proton scattering).⁷ The analyzing power for this reaction is given by curve C in Figure 5. For direct γ production at 90° CM, $a = +0.6$. The 2-spin asymmetry is

$$A_{LL} = \frac{\Delta G}{G} \frac{\Delta q}{q} \hat{a} , \quad (4)$$

where $\Delta G/G$ is the polarization of the initial gluon in the polarized proton, and $\Delta q/q$ is the polarization of the quark. Now, $\Delta q/q$ is A_1 , measured by deep inelastic scattering. For $x_q = .2$, $\Delta q/q = A_1(x_q = .2) = 0.3$.⁸ Therefore,

$$\frac{\Delta G}{G} = \frac{A_{LL}}{.18} \text{ for } x_q = .2, \quad \theta_\gamma = 90^\circ \quad (5)$$

A 1% measurement of A_{LL} for direct γ production gives a 5% measurement of the gluon polarization.

This example illustrates several important points. The analyzing powers are large. We will want to arrange our kinematics to have our "probe" at large x , where deep inelastic scattering shows that the quarks (dominated by u quarks) have a high polarization. We are then sensitive to the gluon polarization, not ΔG but $\Delta G/G$. However, the number of gluons (G) and sea quarks diverge at low x . Therefore, the polarization of gluons and sea quarks will necessarily be small at very low x . Therefore, we emphasize measuring the polarization of gluons and sea quarks at large x . To reach larger x , it is desirable to use lower energy. A very high energy machine is not attractive for these studies. At the same time, the energy must be sufficient to

guarantee that one is scattering quarks and gluons and that the parton model and pQCD applies. For direct γ production and other 2-spin reactions, we plan to use $\sqrt{s} = 200$ GeV. This strikes a balance between sufficient p_T and large x . It is also convenient because the heavy ion program will run proton-proton collisions often at this energy to compare to 100 GeV x A gold-gold collisions. These runs will use polarized protons and the heavy ion studies will average over the spin states.

We have discussed the lowest order pQCD sensitivity to polarization. How do higher order graphs affect this sensitivity? Two groups have studied this for direct photons and Drell-Yan production. Both found that the higher order contributions maintain the sensitivity to polarization.⁹

The STAR Detector

Figure 7 shows the STAR TPC detector. A barrel TPC covers $|\eta| \leq 1$, inside a 0.5 Tesla solenoidal magnetic field. They are constructing a silicon vertex tracker, fast time-of-flight counters outside the TPC, and an electromagnetic calorimeter outside that. About 5 radiation lengths deep, scintillation counter strips (divided both azimuthally and longitudinally) will give information on the spread of the electromagnetic shower. One end cap will expand γ acceptance to $|\eta| \leq 2$. I will discuss STAR's measurement of direct $\gamma +$ jet.

Figure 8 shows a $q + g \rightarrow \gamma + q$ (jet) reaction superimposed on a schematic of part of the STAR detector.

The direct γ showers in EM Cal. I and is seen as one narrow cone by the scintillators between EM Cal I and II. The scintillators in front of I do not see a charged particle and these scintillators and TPC (and vertex chamber which is not shown) assure that the energy is isolated--not part of a jet. A π^0 will typically give two showers in EM Cal I, which show up in the shower maximum detector (the scintillators between I and II) and also be embedded in a jet. The spread of the $\pi^0 \rightarrow 2\gamma$ is $\theta_{\text{open}} = 2m(\pi^0)/E(\pi^0)$. For $p_T > 25$ GeV, the experiment can no longer distinguish γ from π^0 . The large majority of π^0 decay near this minimum opening angle, so that the identification of a direct γ is quite clean. STAR simulation studies give $\pi^0/\gamma = 0.1$ for $p_T = 8-14$ GeV/c.

On the other side, STAR reconstructs the quark jet by combining charged particle momenta as seen by the trackers and electromagnetic energy. This has been studied by STAR. Their resolution is $\Delta E/E(\text{jet}) = 0.25$ for $p_T(\text{jet}) = 30$ GeV/c, and expected efficiency is 80%.

A major complication for STAR is that the drift time of the TPC is very long ((50 μ sec), so that a great many tracks from out-of-time collisions will be seen by the TPC as well as the tracks associated with the triggered event. (The trigger will use energy in the EM Cal, which is a fast detector.) This has been studied and STAR has

developed a strategy for selecting the correct tracks. The basic idea is that out-of-time tracks drift so that they no longer point back to the vertex. The resolution and efficiency include this, for maximum luminosity, ($\sqrt{s} = 200 \text{ GeV}$, $L = 8 \times 10^{31} \text{ cm}^2 \text{sec}^{-1}$).

The following table gives the STAR sensitivity for gluon polarization for different x bins. This table uses a "canonical" running time of 4×10^6 seconds and a luminosity of $2 \times 10^{32} \times (200/500) \text{ cm}^{-2} \text{ sec}^{-1}$ adjusted to $\sqrt{s} = 200 \text{ GeV}$, where we use the fact that the luminosity is proportional to energy. It also assumes a factor 2 reduction in data from event selection, based on a STAR study of isolation cuts and shower studies. The errors are statistical only and do not include background (in fact, expected to be $\leq 10\%$ for these events) or systematic errors (which would include absolute knowledge of the beam polarization and ΔA_1 , from deep inelastic scattering).

Table 1: Error in $\Delta G/G$ from direct $\gamma + \text{jet}$ (STAR)

x (gluon)	$x_q \leq .2$.2 - .3	.3 - .4	$> .4$
0.00 - 0.05	---	0.07	0.06	0.04
0.05 - 0.10	0.04	0.04	0.06	0.07
0.10 - 0.15	0.04	0.06	0.12	0.2
0.15 - 0.20	0.13	0.11	0.2	0.4
> 0.2	---	0.2	0.3	0.4

The PHENIX detector, presented next for W^+ production, will measure direct γ production also. They will use a fine-grained EM calorimeter which can reconstruct π^0 out to $p_T = 25 \text{ GeV}/c$. They do not have the jet acceptance of STAR. Their sensitivity for this and many other reactions will be shown later.

STAR will have excellent sensitivity for gluon polarization from jet production also. (PHENIX does also use π^0 production.) The complication is that several subprocesses contribute to jet production. However, at lower p_T , jet production will be predominantly from gg collisions, and at large p_T (moderate x), gq dominates. Therefore at large p_T , the 2-spin asymmetry A_{LL} will measure

$$A_{LL} \approx \frac{\Delta G}{G} (x_1) \frac{\Delta q}{q} (x_2) \hat{a} (g + q \rightarrow g + q) \quad (6)$$

with an important background from $g + g$. STAR will have a sensitivity of $\delta A_{LL} \approx 0.005$ for $p_T \geq 50$ GeV/c for $\sqrt{s} = 500$ GeV, $L_t = 8 \times 10^{38} \text{cm}^2$.

I discuss the jet production sensitivity because, although the systematic errors from any measurement from this process will be much larger than for direct γ production, the sensitivity to zero gluon polarization will be very significant. Jet production will provide important limits on gluon polarization.

The PHENIX Detector

The PHENIX detector (Figure 9) has two arms covering $|\eta| < 0.35$ with fine grained EM calorimeters (and vertex detector, ring-imaging Cerenkov, and other apparatus shown). These arms each cover 90° in azimuth, left and right. The EM calorimeters are 26,000 channels of 5 cm x 5 cm either lead-scintillator stacks or lead glass at 5 meters from the vertex. The barrel will observe direct γ , π^0 , and electrons (including sign using a 1 Tesla magnetic field from Helmholtz coils). PHENIX also will have two forward/backward muon arms covering the azimuth with $|\eta| = 1.2$ to 2.4. These arms will be used to measure parity-violating W^+ and W^- production, as well as Drell-Yan muon pairs.

Parity violation is a 1-spin longitudinal asymmetry (I won't discuss 2-spin parity violation). We will consider beam 1 as polarized (we average over the spin states of beam 2). Then

$$A_L = \frac{1}{P_1} \frac{N_+ - N_-}{N_+ + N_-} . \quad (7)$$

We will consider W^+ production (Figure 10).

If the W^+ is produced forward (+y) with respect to the polarized proton (note that the protons are not identical!), the production by the Drell-Yan mechanism will favor the u quark from the polarized proton (proton 1) and the d quark from the unpolarized proton (proton 2). This is because for +y, x_1 is large, x_2 small ($x_F > 0$, $x_F = x_1 - x_2$). The u quark dominates at large x, sea quarks (d) are much fewer. Therefore, the parity violation will measure the u-quark polarization for production of W^+ to +y: $A_L (+y) = \frac{\Delta u}{u}$. Likewise, d quark polarization is measured by parity violation for W^+ produced to -y relative to the polarized proton.

However, only the muon is observed from the W^+ decay--can we infer the rapidity of the W^+ from the μ^+ ? The W^+ is left-handed, so that the left-handed ν is emitted in the direction of the W^+ . Therefore, the μ^+ is most favorably emitted backwards from the W^+ , giving a lower energy μ^+ . Referring to Figure 10, a lower energy μ^+ seen in the forward muon detector (forward from the polarized proton)

indicates a W^+ produced to $-y$, and the parity violation measures the \bar{d} polarization. Likewise, a lower energy μ^+ seen in the backward detector measures u polarization.

PHENIX has studied the background for identifying W s. For W^+ , background is mainly $Z \rightarrow \mu^+ \mu^-$ and is 5%. For W^+ , the Z background is 10%. Therefore, W^\pm production is an excellent way to probe quark and antiquark polarization.¹⁰

Figure 11 shows the PHENIX experiment sensitivity for $\Delta u/u$ and $\Delta \bar{d}/\bar{d}$ from W^+ , and their sensitivity for many other measurements of quark and gluon polarizations. We plan to run RHIC at 500 GeV \sqrt{s} with beams polarized longitudinally at PHENIX and STAR for an integrated luminosity of $8 \times 10^{38} \text{ cm}^{-2}$. We also plan to run at $\sqrt{s} = 200 \text{ GeV}$ (parasitically with the heavy ion studies of pp collisions) for $\int L dt = 3 \times 10^{38} \text{ cm}^{-2}$. We assume each beam has 70% polarization. The figure shows the statistical errors expected for quark and gluon polarization. No background has been included either from identifications of the correct reaction or from mixtures of subprocesses. For the reactions shown, this background is expected to be small. (We do not show, for example, the sensitivity to gluon polarization from jet production). No systematic error is included—on knowledge of the beam polarization, for example.

Figure 11 is rather complicated! We just discussed $W^+ \rightarrow \mu^+ + \nu$ parity violation in production. This measurement will be done at $\sqrt{s} = 500 \text{ GeV}$. The measurement of $\Delta d/d$ is shown on the right plot at $x = .24$ with the symbol $W_\mu^+ 500 \text{ PV}$. On the left plot, the point $W_\mu^- \text{ PV}$ shows the $\Delta u/u$ measurement sensitivity. The expected statistical errors are shown (this corresponds to 10000 $W^+ \rightarrow \mu^+ \nu$ events). The different sensitivities are compared to a model from C. Bourrely and J. Soffer which connects polarized and unpolarized structure functions.¹¹ (The curve shown for $\Delta u/u$ is basically A_1 from deep inelastic scattering at large x . The model assumes no \bar{d} polarization, and predicts a large \bar{u} polarization. The larger gluon polarization curve is a parametrization which would “account” for the small amount of the proton spin carried by quarks, as measured by CERN and SLAC.)

$W^- \rightarrow \mu^- + \bar{\nu}$ parity violation in production is sensitive to $\Delta \bar{u}/\bar{u}$ and $\Delta d/d$, and these are shown as $W_\mu^- \text{ PV}$. The parity-conserving W^+ production is a 2-spin asymmetry, proportional to $(\Delta u/u) \times (\Delta d/d)$. Therefore, using the u -quark polarization from DIS (A_1), we can obtain $\Delta \bar{d}/\bar{d}$. This is shown for the PHENIX barrel $W^+ \rightarrow e^+ + \nu$ measurement as $W_e^+ 500 \text{ PC}$. Parity-violating measurements are shown for electrons for $\Delta \bar{u}/\bar{u}$ ($W_e^- \text{ PV}$) and $\Delta u/u$ ($W_e^+ \text{ PV}$).

Gluon polarization measurement sensitivities are shown for direct γ production for PHENIX, $\sqrt{s} = 200 \text{ GeV}$, with the points plotted at $x = 2p_T/\sqrt{s}$, indicated as $\gamma 200$.

Drell-Yan measurements with the muon arms at $\sqrt{s} = 200$ measure $\Delta \bar{u}/\bar{u}$ at the smaller x .

The STAR detector will also measure gluon polarization with great sensitivity (this was given in Table I), $W^\pm \rightarrow e^\pm + \nu$, and $Z \rightarrow e^+ e^-$. We see Z production with

transversely polarized beams as giving a first measurement of the transverse spin parameter $h_1^q(x) \times h_1^{\bar{q}}(x)$. However, this measurement depends on a substantial value for the anti-quark $h_1^{\bar{q}}(x)$. STAR obtains 4000 Zs in $\int L dt = 8 \times 10^{38} \text{ cm}^{-2}$.

Systematic Errors

One important requirement is to know the beam polarization well. For the AGS, we have measured elastic pp scattering at $-t = .3 \text{ (GeV/c)}^2$ from the hydrogen in a nylon string which is spooled through the beam. The analyzing power of this reaction is proportional to 1/momentum, and becomes too small above the AGS energy.

We plan to use inclusive π^- production asymmetry at RHIC. The analyzing power of this reaction is quite large, measured to be $A_N = 0.18 \pm .02$ at Fermilab for a 200 GeV beam, $x_F = .6$, $p_T = 0.09 \text{ GeV/c}$.¹² We chose π^- to avoid needing particle identification. However, the π^+ asymmetry is measured better at both low energy (ZGS) and high (200 GeV), encouraging us to believe that the analyzing power is largely energy independent. We believe that the π^- polarimeter will make an excellent relative polarimeter, measuring the polarization to 8% in less than 1 second (the measuring time depends on whether the measurement is destructive, significantly increasing the emittance through multiple Coulomb scattering). The measurement is only absolute at 200 GeV at this time (to $\Delta A_N/A_N = \pm .1$), since the Fermilab experiment (E704) used polarized protons from a Λ beam for which they could calculate the polarization. We would like to develop an absolute calibration at 100 GeV and 250 GeV. Our primary candidate is Coulomb-Nuclear interference, as proposed by a small-angle scattering RHIC experiment. Our goal is to have a calibration to 5%.

We expect to cancel systematic apparatus effects by frequent reversal of the polarization—every 110 nanoseconds. We will load 114 bunches into each RHIC ring, selecting the polarization sign for each bunch. We plan a pattern (+ - + - etc.) for one ring and (+ + - - etc.) for the second ring. Now, the same bunches collide at a detector for a given fill, so systematic errors can arise from different luminosities for different bunch-bunch collisions. This effect is reduced by averaging over many bunches (114) and over many fills (one fill per day). The experiments will also measure bunch-bunch luminosities. A very nice way to reduce the effect of different luminosities for different spin combinations is to frequently reverse the spin of all the bunches in one ring. This is done by introducing a controlled resonance, and is expected to take 1 second (this has been done at the Indiana Cyclotron)¹³ with very little polarization loss. We believe that systematic apparatus and luminosity effects will be quite small at RHIC.

RHIC Polarized Proton Schedule

The Polarized Collider Workshop at Penn State in November 1990 led to the formation of the RHIC Spin Collaboration.¹⁴ This group has developed the physics case and the accelerator case for the RHIC spin program.

The accelerator team has built and installed a partial Siberian snake in the AGS and verified, in 1994, that the device avoids the 40 "imperfection" spin resonances in the AGS. Future studies will be on "intrinsic" resonances, intensity, and transfer of the polarized beam to RHIC. The AGS snake and AGS polarimeter are installed and work. The team is led by Thomas Roser, with Michael Syphers the Project Manager for RHIC polarized beam. Two prototypes are planned for helical dipole magnets for Siberian Snakes and spin rotators for RHIC and the choice of design will be made fall 1996.

A polarized measurement working group has been formed, led by Yousef Makdisi. This group will develop the relative and absolute polarimeter for RHIC.

The accelerator hardware for spin and an important upgrade for spin for the PHENIX experiment are funded by RIKEN, Japan. With this funding in place, we anticipate installing the spin apparatus in time for spin measurements in the year 2000, consistent with the RHIC turn-on for heavy ion collisions in 1999.

Two spin experiments are approved--STAR and PHENIX. The spin work is to be an integrated part of the physics of each detector. The spokesmen are John Harris, STAR and Shoji Nagamiya, PHENIX.

The role of the RHIC Spin Collaboration at this time is to help develop common theoretical and experimental spin issues, coupling to accelerator issues, and the accelerator team is responsible for the RHIC accelerator spin hardware and commissioning.

Acknowledgments.

The RIKEN initiative, under M. Ishihara, has been crucial to the success of the RHIC spin program. The physics case was developed by many. I would particularly like to mention the work of the Argonne group, led by Aki Yokosawa, and the work of Jacques Soffer of Marseille. Figure 11 was developed by Michael Tannenbaum of Brookhaven and PHENIX.

This work was performed under the auspices of the U. S. Department of Energy.

References

1. Ya. S. Derbenev and A. M. Kondratenko, Sov. Phys. Doklady **20**, 562 (1976); Ya. S. Derbenev *et al.*, Particle Accelerators **8**, 115 (1978).
2. A. D. Krisch *et al.*, Phys. Rev. Lett. **63**, 1137 (1989).
3. V. I. Ptitsin and Yu. M. Shatunov, V Workshop on High Energy Spin Physics, Protvino (1993), S. B. Nurushev, editor.

4. T. Roser, in High-Energy Spin Physics--1988, Minneapolis, edited by K. J. Heller and S. L. Smith, AIP Conf. Proc. No.187, p. 1442.
5. H. Huang *et al.*, Phys. Rev. Lett. 73, 2982 (1994); tests to full energy completed Dec. 1994.
6. C. Bourrely *et al.*, Phys. Rep. 177, 319 (1989).
7. E. L. Berger and J. Qiu, Phys. Rev. D40, 778 (1989).
8. SMC: D. Adams *et al.*, Phys. Lett. B329, 399 (1994); Erratum, Phys. Lett. B339, 332 (1994).
9. Direct γ : A. P. Contogouris *et al.*, Phys. Lett. B304, 329 (1993); L. E. Gordon and W. Vogelsang, Phys. Rev. D49, 170 (1994). Drell-Yan: A. P. Contogouris *et al.*, Phys. Rev. D48, 4092 (1993).
10. E. Leader, Phys. Rev. Lett. 56, 1542 (1986).
11. C. Bourrely and J. Soffer, Nucl. Phys. B445, 341 (1995).
12. D. L. Adams *et al.*, Phys. Lett. B264, 462 (1991).
13. R. A. Phelps, Proc. Third Workshop on Siberian Snakes and Spin Rotators, A. Luccio and Th. Roser, editors, Brookhaven National Laboratory Report BNL-52453, p. 15 (1994).
14. J. Collins, S. Heppelmann and R. W. Robinett (editors), Proc. Of the Polarized Collider Workshop, Pennsylvania State University (1990), AIP Conf. Proc. No. 223, New York (1991). The RHIC Spin Collaboration: H. Spinka, D. Underwood, A. Yokosawa (Argonne National Laboratory); G. Bunce, E. Courant, R. Fornow, H. Huang, Y. Y. Lee, D. Lowenstein, A. Luccio, Y. Makdisi, L. Ratner, T. Roser, M. Syphers, M. Tannenbaum (Brookhaven National Laboratory); V. Ptitsin, Yu. Shatunov (BINP); J. B. Carroll, T. Hallman, G. J. Igo (UCLA); N. Törnqvist (Helsinki); S. Y. Lee (Indiana); A. S. Akimenko, Yu. I. Arestov, N. I. Belikov, V. I. Belousov, B. V. Chujki, A. M. Davidenko, A. A. Derevschikov, S. V. Erin, A. A. Grachov, A. S. Konstantinov, I. V. Kotov, Yu. A. Matulenko, A. P. Meschanin, N. G. Minaev, A. I. Mysnick, S. B. Nurushev, A. I. Pavlinov, A. Yu. Polyarush, A. I. Ronzhin, V. L. Rykov, V. A. Sergeev, K. E. Sheshtermanov, L. F. Soloviev, O. D. Tsay, A. G. Ufimtsev, A. N. Vasiliev (IHEP); I. G. Alekseev, V. P. Kanavets, B. V. Morozov, V. M. Nesterov, D. N. Svirida (ITEP); N. Akchurin, Y. Onel (Iowa); A. Bravor, M. Conte, A. Penzo, M. Pusterla, P. Schiavon (Italy); L. Madansky, R. Welsh (Johns Hopkins); S. Hiramatsu, T. Mori, H. Sato (KEK); H. Enyo, K. Imai, A. Masaike (Kyoto); M. Werlen (Lausanne); G. A. Agakishiev, G. S. Averichev, A. M. Baldin, A. E. Dorokhov, A. V. Efremov, N. I. Kochelev, A. M. Kondratenko, A. D. Kovalenko, E. A. Matyushevskii, Yu. I. Minaev, N. S. Moroz, J. J. Musulmanbekov, Yu. A. Panebratsev, N. M. Piskunov, S. V. Razin, N. V. Slavin, S. S. Shimanskiy, E. A. Strokovsky, O. V. Teryaev, M. V. Tokarev, V. I. Yurevich (LHE-JINR); J. Soffer (Marseille); R. Jaffe, X. Ji (MIT); E. A. Atkin, V. V. Grushin, A. V. Khodinov,

D. V. Kostin, A. N. Lebedev, S. V. Lubyanov, A. N. Nazarov, V. N. Nevolin, A. S. Oltchak, E. M. Onishenko, D. M. Penzin, A. V. Shalnov, A. B. Simakov, M. N. Strikhanov, Yu. I. Sytsko, A. A. Valnyashin, Yu. A. Volkov, S. A. Voloshin, V. E. Zyrin (MEPhI); J. Collins, S. Heppelmann, R. Robinett (Penn State); A. P. Potylitsin, G. M. Radutsky, A. N. Tabachenko, I. V. Glavanakov, Yu. F. Krechetov, A. V. Moiseenko, E. N. Shuvalov, N. P. Fedorov (Tomsk Nuclear Physics Institute); T. Ichihara, M. Ishihara, N. Saito, Y. Watanabe (Riken Institute); T.-A. Shibara (Tokyo Institute of Technology); J. M. Moss, J. McClelland (Los Alamos National Laboratory).

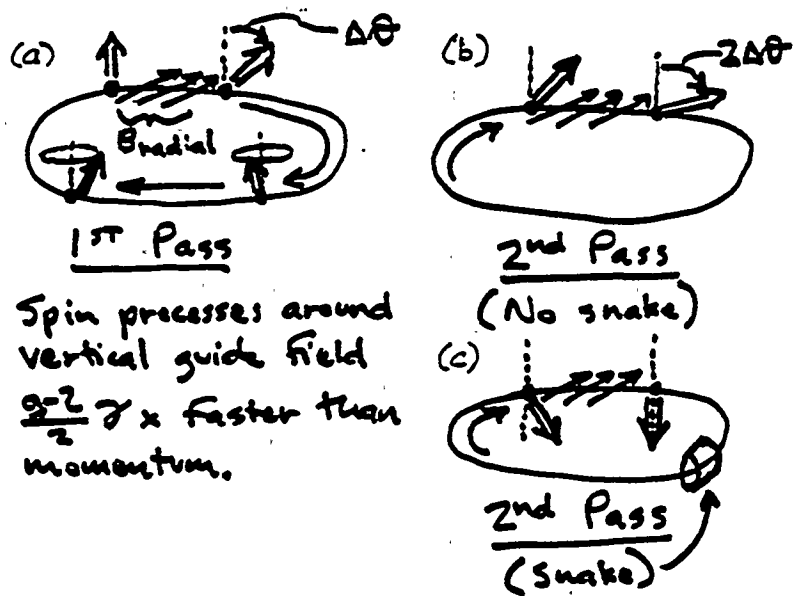


Figure 1.

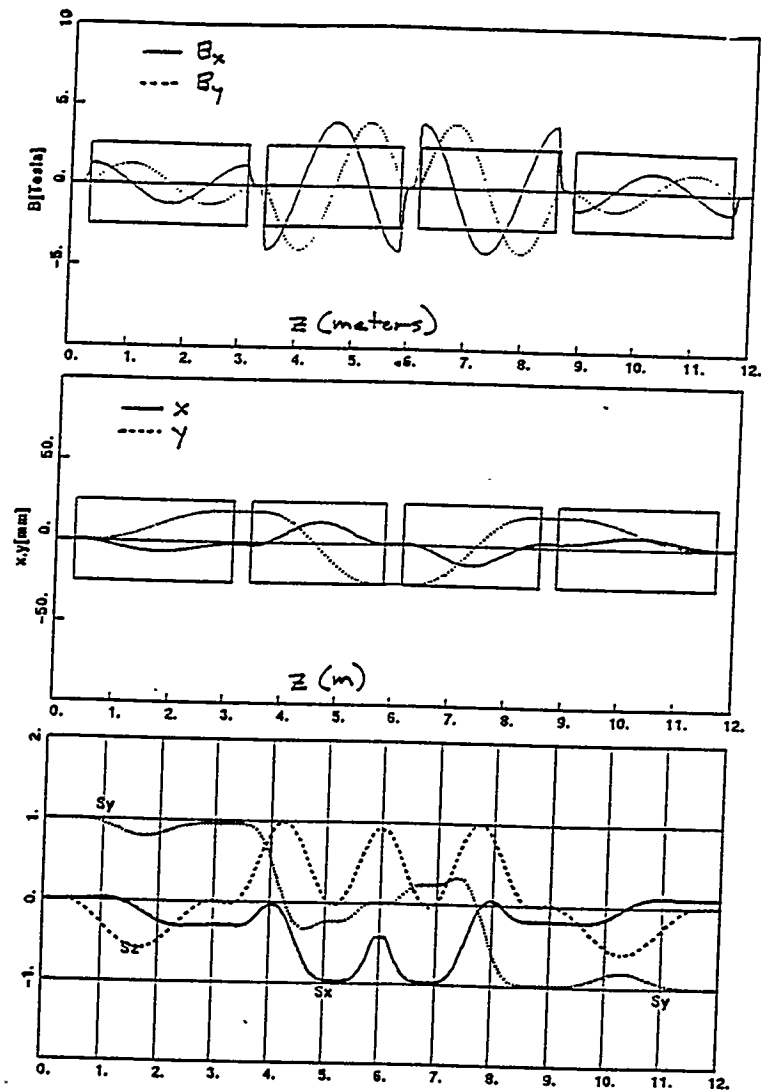


Figure 2.

Polarized Proton Collisions at Brookhaven

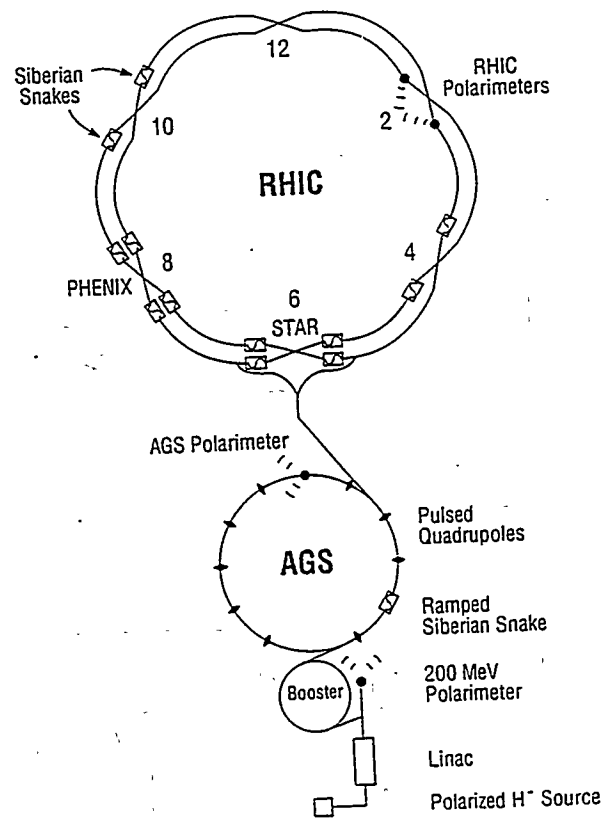
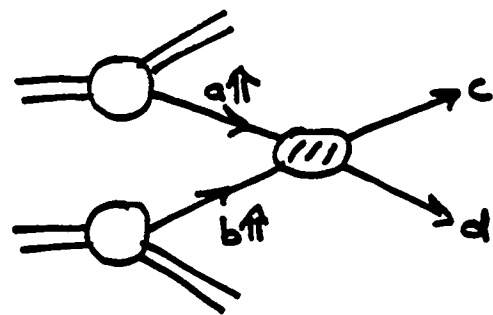


Figure 3.



$$A_{LL} \sim \frac{\Delta a}{a} \frac{\Delta b}{b} \hat{a}(a+b \rightarrow c+d)$$

Figure 4.

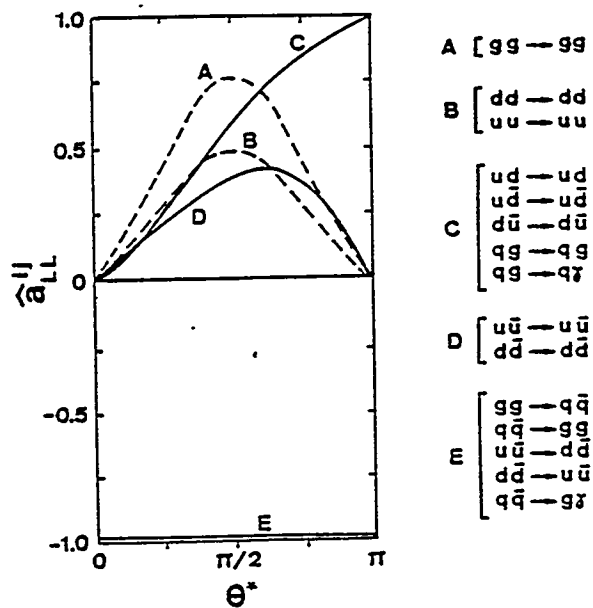


Figure 5.

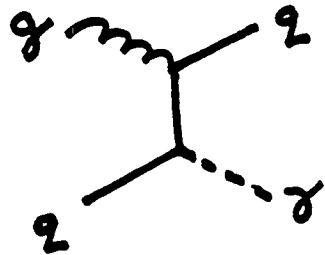


Figure 6.

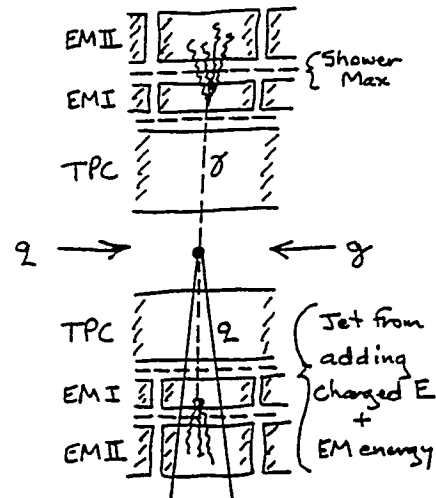


Figure 8.

STAR Detector

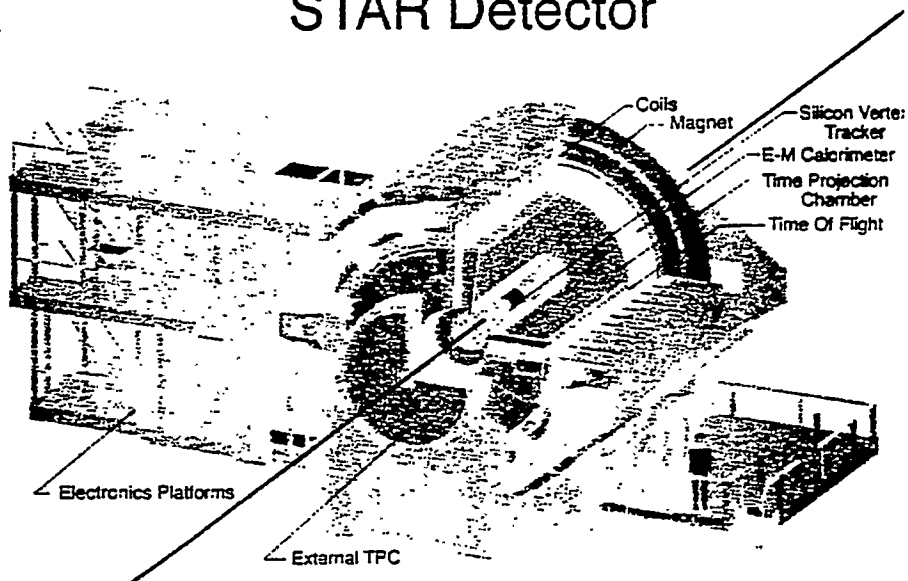


Figure 7.

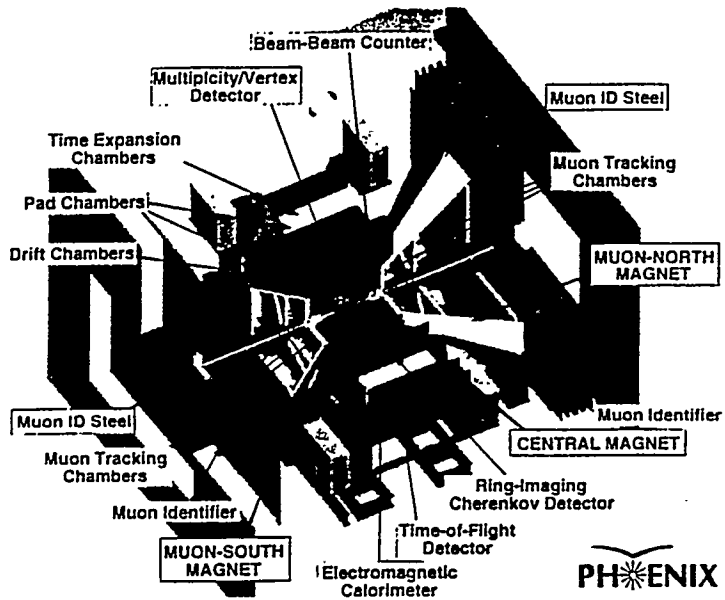
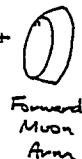


Figure 9.

- ① $p_1 \uparrow p_2$ collision: $p_1 \xrightarrow{\text{Polarized}} \leftarrow p_2$ Unpolarized
- ② \bar{d}, u_2 collision: $\bar{d}_1 \leftarrow \leftarrow u_2$
- ③ W^+ produced backward: $W^+ \leftarrow \leftarrow$
- ④ $W^+ \rightarrow \mu^+ \nu$, left-handed ν in direction of W^+ , lower energy μ^+ in forward muon arm



The forward production of a lower energy μ^+ measures the \bar{d} polarization in the polarized proton.

Figure 10.

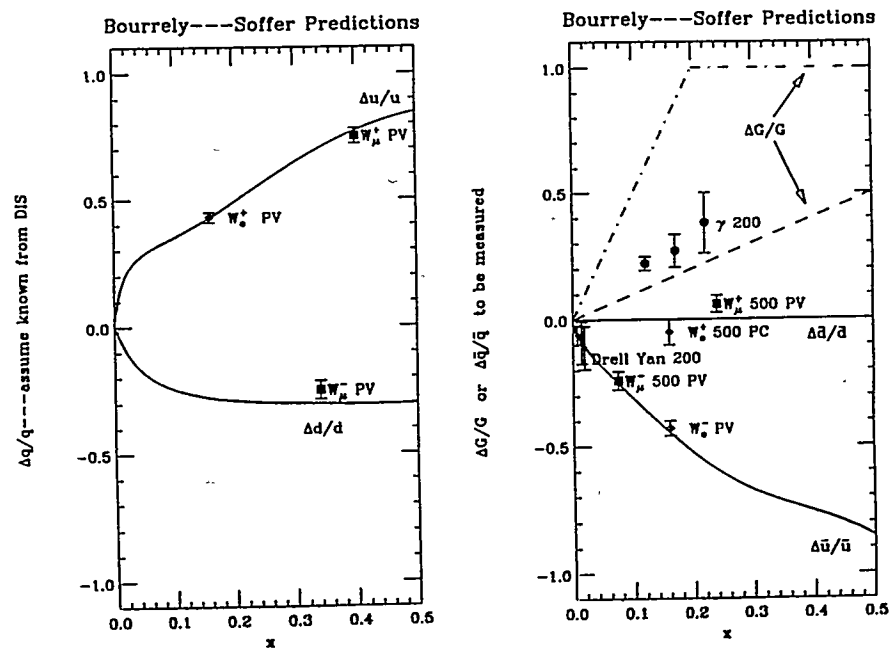


Figure 11.